Intranasal insulin affects brain, but not peripheral tissue, glucose uptake in lean, healthy men - a positron emission tomography study

Aino Latva-Rasku[1] (0000-0001-8786-9160),
Sanna Laurila[1,2] (0000-0002-1170-5079),
Tomi Karjalainen[1] (0000-0002-8181-9493),
Riku Klén[1] (0000-0002-0982-8360),
Eliisa Löyttyniemi[3] (0000-0002-7278-6511),
Olli Eskola[1] (0000-0002-9874-5662),
Lauri Nummenmaa[1,7] (0000-0002-2497-9757),
Martin Heni[4,5,6] (0000-0002-8462-3832),
Pirjo Nuutila[1,8] (0000-0001-9597-338X)

[1]Turku PET Centre, University of Turku, Turku, Finland
[2]Turku Heart Center, Turku University Hospital, Turku, Finland
[3]Department of Biostatistics, University of Turku, Turku, Finland.
[4] Department of Internal Medicine I, Division of Endocrinology and Diabetology, Ulm University Hospital, Ulm, Germany.
[5] Institute for Clinical Chemistry and Pathobiochemistry, University Hospital Tübingen, Tübingen, Germany
[6] Institute for Diabetes Research and Metabolic Diseases, Institute for Diabetes Research and Metabolic Diseases of the Helmholtz Center Munich at the University of Tübingen, Tübingen, Germany
[7]Department of Psychology, University of Turku, Finland
[8]Department of Endocrinology, Turku University hospital, Turku, Finland

Word count: Abstract: 194, Main text: 3617, References: 43, Tables: 1, Figures: 4

Correspondence:
Aino Latva-Rasku, MD, PhD
e-mail: aino.e.latva-rasku@utu.fi

ABSTRACT

Aims To study the effects of intranasal insulin on brain and peripheral tissue-specific glucose uptake, and systemic lipid concentrations in lean, healthy males.

Methods On two separate visits, ten subjects received either 160 IU intranasal insulin (INI) or placebo during a low-dose hyperinsulinemic (0.25 mU kg^{-1} min^{-1}), euglycaemic clamp in a randomised, single-blinded, crossover design. Tissue glucose uptake was quantified using positron emission tomography (PET) and glucose analogue tracer 2-deoxy-2[^{18}F]fluoro-D-glucose ([^{18}F]-FDG), with a dynamic scan performed from 40 to 90 minutes and covering major insulin sensitive tissues. Serum lipid samples were collected at fasting, at the moment of spray application, and 60 minutes and 90 minutes following sprays.

Results INI induced a global decrease in brain glucose uptake in all subjects. While INI had no effect on skeletal muscle or adipose tissue glucose uptake, median hepatic glucose uptake increased by 43 % in insulin sensitive (Matsuda-ISI ≥7.4) subjects without affecting EGP. Serum lipid profile remained unaffected.

Conclusions A single dose of 160 IU intranasal insulin decreased brain glucose uptake globally 40 min after administration, possibly indicating a transient excess of glucose uptake before the time of [^{18}F]-FDG injection. Hepatic glucose uptake was only enhanced in very insulin sensitive subjects suggesting an early disruption of central regulation, while no changes were observed in other peripheral tissues, endogenous glucose production or circulating lipids.

Trial registration ClinicalTrials.gov NCT02933645.

Keywords: intranasal insulin, insulin sensitivity, positron emission tomography, tissue glucose uptake

RESEARCH IN CONTEXT:

What is already known about this subject?

- Intranasal insulin sprays have been shown to cause widespread changes in peripheral glucose metabolism in animal models
- In humans acute intranasal insulin application has been shown to suppress endogenous glucose production, whereas results on other tissues have shown variable results

What is the key question?

- Does intranasal insulin administration affect glucose uptake in skeletal muscle, liver, adipose tissue and the brain in lean, healthy male human subjects?

What are the new findings?

- In the current study intranasal insulin did not affect endogenous glucose production or peripheral glucose uptake under mild systemic hyperinsulinemia except in the very insulin sensitive, lean healthy males, where it promoted liver glucose uptake
- Brain glucose uptake rate measured 40 to 90 min was decreased after intranasal insulin application

How might this impact on clinical practice in the foreseeable future?

- Our results suggest that the brain can be capable of regulating liver glucose metabolism in humans, but this interplay is disrupted early on in the development of insulin resistance.

INTRODUCTION

In recent years defective insulin signalling and glucose homeostasis in the central nervous system (CNS) have been associated extensively with metabolic diseases, particularly type 2 diabetes (T2D) and obesity. Furthermore, brain insulin resistance is thought to be linked to neurocognitive decline. Details on the role of CNS insulin receptor activation in the regulation of peripheral insulin sensitivity and glucose metabolism have been comprehensively reviewed (Kullmann 2020, Scherer 2021).

Studies in rodents have shown that functioning insulin signalling in the medial hypothalamus is crucial for the regulation of both endogenous glucose production (EGP) (Obici 2002, Pocai 2005), as well as for white adipose tissue lipolysis and lipogenesis in rodents (Koch 2008, Scherer 2011). While increased whole-body glucose consumption after hypothalamic insulin receptor activation is frequently attributed to a significant decrease in EGP with no significant effect on other peripheral tissues (Pocai 2005), increased skeletal muscle glycogen synthesis (Perrin 2004) and muscle glucose uptake (Coomans 2011) have also been reported in rodents. However, a carefully planned study in dogs failed to reproduce the results on central regulation of EGP, showing only a modest suppression of net hepatic glucose output resulting mostly from enhanced glucose uptake and glycogen synthesis (Ramnanan 2011).

Central effects of insulin have been studied in humans using intranasally administered insulin (INI). When spraying up the nose, insulin reaches the brain via the olfactory nerve tracts, bypassing the blood-brain barrier, as demonstrated in mice (Renner 2012). The existence of such direct route in humans has been endorsed by studies that demonstrated rapid changes in cerebro-spinal fluid (CSF) insulin concentration (Born 2002) and brain activation (Heni 2014) with only minimal changes in circulating insulin levels. Using INI, Heni et al. reported increased glucose infusion rates during low-dose hyperinsulinemic, euglycaemic clamp starting 40–60 minutes after INI administration in healthy, lean males (Heni 2014 and 2017), as well as a more delayed (190–210 min after INI) increase in glucose rate of disappearance (Heni 2017). In line with animal studies, INI has been shown to have a suppressing effect on EGP during systemic hyperinsulinemia (Dash 2015, Heni 2017), although the timeframe of the possible effect differs in these two studies, as they used different methods. Despite precipitating hypothalamic activation (Heni 2014 and 2017), INI does not seem to influence EGP during fasting (Gancheva 2015, Plomgaard 2019). Thus, hepatic insulin action might be necessary for brain-derived effects on liver glucose metabolism, hence, brain signals might enhance direct insulin action at the liver.

In addition to glucose metabolism, insulin administered to the brain has been shown to reduce lipolysis in mice, possibly via lowered sympathetic nervous system (SNS) activity in visceral adipose tissue (Scherer 2011). Inhibition of lipolysis by INI has also been demonstrated in humans (Iwen 2014), however, this has not been replicated in studies with elevated circulating insulin concentrations . Hence the relevance of these findings for human physiology is still under debate.

We now aimed to clarify, if brain insulin action stimulates glucose uptake in lean humans and if so, where this might occur. We therefore quantified the effects of INI on tissue-specific glucose uptake (GU), primarily in skeletal muscle, liver, and subcutaneous and brown adipose tissue in lean, healthy male subjects by facilitating positron emission tomography (PET) and a glucose analogue tracer 2-deoxy-2-[^{18}F]fluoro-D-glucose ([^{18}F]-FDG) together with a low-dose hyperinsulinemic, euglycaemic clamp (DeFronzo 1979, Heni 2014). The effect on systemic lipid metabolism was also investigated post hoc from serum samples. We hypothesised that INI could increase GU in peripheral tissues, as well as suppress EGP and lipolysis.

MATERIALS AND METHODS

PET study subjects

Ten healthy, normal weight male subjects not taking any medications, and with normal glucose tolerance based on 75 g oral glucose tolerance test, and fasting insulin levels within the hospital reference range were enrolled in the study. To test the effect of peripheral insulin sensitivity on response to INI, the group was further divided into two based on the median of Matsuda-ISI (≥7.4 in high and <7.4 in impaired insulin sensitivity group). Body fat percentage was measured using bioimpedance (Omron BF400 [MBF-400-E], Omron Healthcare Co Ltd, Kyoto, Japan).

PET study protocol

The study was performed in a randomised, single-blind, crossover design. The subjects received either 160 IU intranasal insulin or placebo under mild systemic hyperinsulinemia and euglycaemia before a whole-body [^{18}F]-FDG PET scan on two separate study visits 2–16 days apart. The study protocol was approved by Finnish Medicines Agency Fimea and the Southwest Finland Hospital District Independent Ethics Committee. All subjects gave written informed consent before any study procedures. The study was registered at ClinicalTrials.gov (Identifier: NCT02933645).

The protocol of scan visits is summarised in Figure 1. The visits started with the insertion of two venous catheters in opposite forearms, one for infusion of insulin and glucose and injection of [^{18}F]-FDG, and other for collection of venous blood samples, arterialised by placing a hot water bottle distally on the arm. After collection of fasting plasma blood samples, a low-dose hyperinsulinemic, euglycaemic clamp was started with a bolus of 6.25 mU/kg over 7 minutes and continued with a dose of 0.25 mU kg^{-1} min^{-1} human insulin (Actrapid, Novo Nordisk A/S, Bagsvaerd, Denmark) (DeFronzo 1979, Heni 2014). Euglycaemia was maintained with a variable rate infusion of 20% glucose based on plasma glucose measurements performed every 5–10 min.

The nasal insulin sprays were administered 30 minutes after the start of clamp on both visits as 8 puffs in each nostril over 4 minutes. To simulate the spillover of insulin into systemic circulation previously seen with intranasal insulin administration, the subjects received an intravenous insulin bolus of 2.5 mU/kg over 15 minutes together with placebo sprays. (Heni 2017, Plomgaard 2019)

40 min (SD 6) after administration intranasal insulin or 39 min (SD 9) after placebo the subjects were injected with [^{18}F]-FDG (187 MBq [SD 9] after insulin sprays; 181 MBq [SD 10] after placebo sprays), manufactured as described earlier (Hamacher 1986). The combined PET/CT scan (Discovery 690; General Electric Medical Systems, Milwaukee, WI) was started right after, with thoracic area (40 min), upper abdomen (15 min), thighs (15 min), neck (10 min) and the brain (10 min) scanned sequentially in the same session, and with the clamp continuing until the end of scan. Amount of [^{18}F]-FDG lost into urine was measured from a urine sample given at the end of scan using an isotope dose calibrator (Model VDC-205, Comecer Netherlands, Joure, Netherlands).

Nasal insulin and placebo sprays

Spray bottles containing either intranasal insulin (100 IU/ml, Actrapid, Novo Nordisk A/S, Bagsvaerd, Denmark), or placebo (Insulin Diluting Medium for Novorapid and Levemir, Novo Nordisk A/S, Bagsvaerd, Denmark) were manufactured by the local hospital pharmacy. The sprays were administered to the subjects in a single-blinded fashion, and in an order randomised in blocks with all subjects undergoing both interventions.

Analysing peripheral tissue GU from PET data

Before analysis, all PET data was corrected for dead time, decay and photon attenuation. Input function was obtained by combining activity data from PET images from inside the left ventricle (first 10 minutes), and plasma samples collected at nine time points during the scan and analysed with an automated gamma counter (Wizard 1480 3, Wallac, Turku, Finland). Tissue activity was determined using Carimas software (Version 2.9, Turku PET Centre, downloadable at http://www.turkupetcentre.fi), applying free-hand drawn region of interests for other tissues: both quadriceps femoris muscles, portion of right lobe of the liver, supraclavicular brown adipose tissue depots, and several smaller volumes of abdominal subcutaneous adipose tissue. The acquired time-activity curves from different tissues and blood were then compared to determine tracer uptake using the Patlak-Gjedde plot (K_i) (Patlak 1985) or its estimate, fractional uptake rate (FUR) (Ishizu 1994).

Next, tissue GU (μmol kg^{-1} min^{-1}) was calculated by multiplying K_i or FUR with plasma glucose level, and dividing by tissue density and a constant accounting the differences in metabolic rates of [^{18}F]-FDG and glucose (1.2 for skeletal muscle, 1.0 for liver, 1.14 for adipose tissue, 0.65 for brain) (Peltoniemi 2000, Iozzo 2007, Virtanen 2001, Wu 2003).

EGP was calculated by subtracting the amount of glucose infused after injection from the whole-body glucose disposal rate (Rd) derived from [^{18}F]-FDG consumption (Iozzo 2006).

Quantifying brain GU

Glucose uptake in the brain was obtained using SPM12-based toolbox Magia (Karjalainen 2020), with GU calculated from FUR results. The data were then spatially normalised to MNI space using an in-house [^{18}F]-FDG template and finally smoothed with a Gaussian kernel with 8-mm full-width at half-maximum.

Serum metabolites

Serum samples were collected from the first nine subjects and used for comprehensive analysis of metabolites at Nightingale Health Ltd laboratory, using nuclear magnetic resonance (NMR) (Soininen 2009), with the focus on serum total fatty acids, glycerol, triglycerides in VLDL, LDL and HDL as well as total serum triglycerides, and apolipoproteins A-I and B. Samples were collected at fasting, during clamp prior to nasal spray administration, as well as 60 and 90 minutes after administration.

Statistical analyses

The sample size was determined to detect a 22% placebo-corrected change in glucose infusion rate, based on unpublished results from Tübingen, with 95% power at a two-tailed significance level of 5%. Baseline characteristics were compared using independent samples t-test. Analysis for changes in tissue GU were performed using a mixed model for repeated measurements with fixed effects of intervention, period, sequence (=intervention order). The results are reported as INI-induced mean changes compared to placebo with a 95% confidence interval (CI). Changes in brain GU were estimated using paired t-test in SPM12, with $p<0.05$ as the cluster-defining threshold. Only statistically significant clusters ($p<0.05$, FWE-corrected) are reported. For serum metabolites, changes from spray application to 60 and 90 minutes later were compared between interventions using paired Wilcoxon signed rank test with Rstudio (RStudio Inc., Boston MA).

RESULTS

Participant characteristics

Baseline measurements made on the screening visit are presented in Table 1. The subgroup with higher insulin sensitivity were older ($p=0.003$), had lower fasting insulin levels ($p=0.02$) and higher

Matsuda-ISI (p=0.04) than the impaired insulin sensitivity group, but there was no difference between groups in weight, BMI, fat percentage, waist-hip ratio, or fasting plasma glucose and HbA1c levels.

INI effects on plasma glucose and insulin during clamp

Plasma glucose values were comparable and within euglycaemia during both interventions (Figure 2A). While the spillover of minor amounts of INI into the circulation was well mimicked by an iv insulin infusion on placebo day, serum insulin levels were numerically higher after INI from 25 minutes after the sprays until the end of study (Figure 2B). However, the difference in mean insulin levels after spray application did not reach statistical significance (19.4 pmol/L, 95% CI -2.0, 40.8, p=0.07), and the degree of change in insulin levels did not correlate with tissue GU results.

Suppressed brain GU after INI

GU was extensively decreased in all brain areas after INI administration when analysing the whole group (Figure 3), with no significant differences between different anatomical brain regions. There was no difference in GU between groups after placebo sprays, or in the magnitude of change between groups.

No effect on whole-body or skeletal muscle GU

Glucose infusion rates (GIR) tended to increase towards the end of the study after INI, but the change was not statistically significant (Figure 2C) (at the time of maximal difference at 120 min 0.9 mg kg^{-1} min^{-1}, 95% CI -0.2, 1.9, p=0.09). Furthermore, rate of total tracer-derived glucose disappearance (Rd) during the scan was not altered by INI (2.4 µmol kg^{-1} min^{-1}, 95% CI -1.3, 6.1, p=0.17) (Figure 4A). In line with this, skeletal muscle GU was not affected by INI (0.3 µmol kg^{-1} min^{-1}, 95% CI -1.8, 2.5, p=0.75) (Figure 4A), and there was no significant difference between subjects with high or impaired insulin sensitivity.

Enhanced liver GU only in insulin sensitive subjects, no change in EGP

In the whole group INI did not increase GU into liver (1.0 µmol kg^{-1} min^{-1}, 95% CI -1.6, 3.7, p=0.39) or affect EGP (-2.5 µmol kg^{-1} min^{-1}, 95% CI -6.3, 1.2, p=0.16) (Figure 4A). However, in the high insulin sensitivity group INI induced a significant 43 % median increase in liver GU (+5.6 µmol kg^{-1} min^{-1}, 95% CI 1.3, 9.8, p=0.02) (Figure 4B), but had no effect on EGP (-4.1 µmol kg^{-1} min^{-1}, 95% CI -10.0, 1.8, p=0.15). In comparison, liver GU tended to be lower after INI in subjects with impaired insulin sensitivity (-3.5 µmol kg^{-1} min^{-1}, 95% CI -7.8, 0.7, p=0.09) (Figure 4B).

Unaffected adipose tissue GU

There was no significant changes in waist subcutaneous adipose tissue (0.2 µmol kg^{-1} min^{-1}, 95% CI -1.5, 1.9, p=0.79) or BAT GU (-1.09 µmol kg^{-1} min^{-1}, 95% CI -13.4, 11.2, p=0.83) in response to INI regardless the level of peripheral insulin sensitivity (Figure 4A). One subject was excluded from BAT analysis due to abnormal activation of the tissue on the placebo visit, although including him would not have changed the result.

Serum lipids

Levels of serum total fatty acids, glycerol, triglycerides in VLDL, LDL and HDL, total triglycerides, or apolipoproteins A-I and B were not significantly affected by INI. The results are detailed in supplementary figures 1 and 2.

DISCUSSION

Our study shows that a single dose of intranasally administered insulin reduces brain glucose uptake measured with [^{18}F]-FDG-PET under mild systemic hyperinsulinemia in lean, healthy male subjects,

but enhances hepatic glucose uptake only in insulin sensitive subjects. We did not observe changes in whole-body, skeletal muscle or adipose tissue glucose uptake, or in serum lipid concentrations in response to INI.

Globally lower cerebral glucose uptake after INI has not been reported earlier in humans, with the majority of research focusing on functional effects and effects on peripheral metabolism rather than metabolism of the brain itself. However, in line with the current results, INI has been shown to induce a global decrease in brain glucose uptake during fasting in healthy mice (Sanguinetti 2019).

As increasing peripheral insulin levels during hyperinsulinemic euglycaemic clamp has been shown to increase brain glucose uptake by 3–4 % (not statistically significantly) compared to fasted state in healthy subjects (Hirvonen 2011), or up to 15 % while suppressing endogenous insulin secretion with somatostatin (Bingham 2002), the 3.3–5.1 % decrease seen in the current study is likely dependent on the route of insulin administration, as well as the timing of [^{18}F]-FDG injection. Although the magnitude of the decrease is not large, within-subject variability of brain glucose utilisation has been shown to be even less in a reproducibility study by Bartlett et al (1988).

It is possible that insulin, that reaches the CNS 10–40 min after INI administration (Born 2002), causes widespread neuronal activation resulting in initial increase in neuronal glycolysis (Diaz-Garcia 2017), and in the recovery phase glia cell-derived lactate produced during the activation might become the preferred fuel source (Diaz-Garcia 2017) in the expense of glucose and [^{18}F]-FDG when the tracer is administered 40 min after INI. Moreover, it has been shown that brain glycogen content decreases within 15 minutes of activation and slowly recovers within the next hour, indicating that glycogenolysis might also serve as another source for glucose or lactate during the recovery period (Dienel 2002). Interestingly a similar decrease in brain [^{18}F]-FDG uptake has been shown to follow peroral glucose administration (Ishibashi 2016).

Alternatively, it is also possible that the effects of INI on brain glucose uptake are, instead of or in addition to neuronal activation, a direct effect of insulin on cellular insulin-mediated glucose metabolism. Insulin has been shown to increase GLUT4 transportation to the plasma membrane in neurons and stimulate GU *in vitro* (Benomar 2006) and in mice (Reno 2017), and promote glycogen synthesis, but not GU, in astrocytes *in vitro* (Heni 2011), so it is possible that these metabolic changes induce a similar decrease in glucose uptake demand as neuronal activation.

Although the cellular mechanisms behind the decrease in brain GU seen in the current study remain elusive, the observed change are in accordance with previous reports. Interestingly, INI has been demonstrated to reduce appetite and food intake in several studies (reviewed by Kullmann et al [2020]), and to increase brain ATP and phosphocreatinine levels already 10 minutes after administration with the effect lasting at least 50 minutes (Jauch-Chara 2012). Therefore, we suggest that the decrease in glucose uptake 40 minutes after INI administration is likely a result of decreased demand for glucose in the brain, and that meeting, or exceeding, central energy needs might also contributes to the anorexigenic effects of INI.

Contrarily to the brain, we did not observe changes in peripheral tissue-specific glucose uptake, so this does not seem to explain the previously reported slight increase in glucose infusion rates starting from 40 minutes after administration (Heni 2014, Heni 2017). However, as whole-body glucose disposal was not affected by INI in our study, it is not unexpected that tissue-specific uptake remained largely unaffected, with rates of GU and EGP resembling fasting rather than insulin-stimulated levels, even despite the higher circulating insulin levels after INI. Currently only one study in mice has reported increased directly measured GU in skeletal muscle during clamp conditions with no effect

on GU in other tissues (Coomans 2011), while other studies report no effect in any peripheral tissue (Scherer 2011). Therefore, it seems that the previously reported effects of INI on whole-body glucose disposal occurs mainly in response to other changes in glucose metabolism, possibly by suppressing EGP.
The method used to measure EGP in the current study only provides an average over the entire duration of the scan (app. 40–120 minutes post sprays). This approach does not have verified capabilities to detect changes that might occur towards the end of this timeframe. Consequently, the absences of observed changes in EGP does not contradict prior research that combined insulin spray and systemic insulin administration. These earlier studies documented decreases in EGP 100 to 120 minutes or 3 to 6 hours after administration of human insulin (Heni 2017) or an insulin analogue (Dash 2015). Hence, our findings remain consistent with this existing body of literature.

Finding increased hepatic glucose uptake in the more insulin sensitive subjects without a change in EGP is in line with findings in dogs by Ramnanan et al (2011), although the changes in the current study occurred at a time point where no effect was yet seen in the previous report in dogs. Furthermore, it remains open how the observed effect is mechanistically mediated. Also, considering the small sample size and the unphysiological portal insulin gradient, these results should be interpreted with care, albeit it is intriguing if a disruption of centrally mediated liver glucose metabolism can be seen this early in the development of insulin resistance. Furthermore, seeing no significant effect on skeletal muscle or whole-body glucose uptake provides support for the possibility of a direct central regulation of hepatic glucose uptake, instead of just confounding effects of insulin spillover that we furthermore corrected for by mimicking iv insulin administration on placebo spray day.

Intracerebroventricular insulin administration has been shown to induce BAT thermogenesis via SNS activation in fasted mice (Rahmouni 2004), and activation of SNS by melanocortin receptor signalling has been shown to increase BAT glucose uptake during fasting in mice (Morgan 2015), but these effects have not been studied in larger mammals. In the current study, brown adipose tissue glucose uptake remained unchanged. Benedict et al. (Benedict 2011) have previously reported that the mean increase in energy expenditure of 2.5 hours increases after INI, while the differences in separate 30 min intervals did not reach statistical significance, and possible spillover after placebo administration was not accounted with intravenous insulin. Therefore, the limited timeframe can also be the reason we did not observe any effect in the current study.

Decreased lipolysis and lipogenesis following insulin administration to the brain, more specifically mediobasal hypothalamus, has been demonstrated in mice as reduced rate of appearance of glycerol during pancreatic clamp (Scherer 2011). Transient lowering of glycerol appearance has also been reported in humans 0–60 minutes after INI administration during fasting (Iwen 2014), while glycerol levels in circulation and subcutaneous WAT interstitium remained unchanged (Gancheva 2015, Iwen 2014). In the current study, we observed no significant changes in serum glycerol, although it tended to decrease with INI compared to placebo, in line with previous studies. We observed no change in serum triglycerides, apolipoproteins or total fatty acids, which is also in agreement with previous studies during fasting (Iwen 2014, Gancheva 2015) and pancreatic clamp with constant fed state (Xiao 2017). The relevance of brain-derived signals on lipolysis in contrast to direct effects of insulin on adipocytes under physiologic circumstances remain under discussion, our current results argue against a major contribution.

While the strengths of this study are the established methods and site experience in measuring tissue GU quantitatively using PET, the approach also has limitations. Assessment of tissue GU is limited to the moment of injection, after which most of the tracer available is trapped within cells during the

first 10 minutes, so this study covers mainly only the effects 40–50 minutes after INI administration and might have missed possible effects at other time points. However, we closely aligned our protocol to earlier reports on the timepoints of insulin action in humans. The increase in CSF insulin concentration starts to occur within 10 minutes (Born 2002), hypothalamic activation can be seen at 30 minutes (Heni 2014), and an increase in GIR needed to sustain euglycaemia starts 40 minutes after INI administration (Heni 2014). A relevant later effect within 120 minutes from spray application seems unlikely as we did not see a significant increase in GIR towards the end of the study. This is supported by a finding that central K_{ATP} channel activation significantly suppresses EGP, but has no effect on glucose rate of disappearance or GIR after 6 hours of administration during pancreatic clamp (Esterson 2016).

Also, compared to previous studies (Heni 2014), the subjects in the current study had higher BMI, and it has been shown that the effects of INI seem to diminish in obese subjects (Heni 2014, Xiao 2018). However, the subjects with higher BMI were mostly also more insulin sensitive, likely due to higher muscle mass, and there was no indication of higher visceral adiposity. Furthermore, the small sample size and including only males does limit generalising the results.

To conclude, we found that 40 minutes after INI administration brain glucose uptake is significantly reduced, possibly as a result of energy needs already being fulfilled rapidly after insulin exposure. Contrary to some previous reports we found no change in peripheral tissue or whole-body glucose uptake, or EGP in the whole group. However, the timeframe of the current study differs from earlier reports and does not contradict the possible later effects on hepatic glucose output. Interestingly, liver glucose uptake was increased only in very insulin sensitive subjects, indicating a possible early disruption of central regulation in the development of systemic insulin resistance, although the small sample size may limit the interpretation. Alterations in brain glucose metabolism after INI should be investigated further to characterise more acute effects of central insulin exposure, but our results confirm that INI has direct central effects, independent of systemic insulin levels.

ACKNOWLEDGEMENTS

The study was conducted within the Finnish Center of Excellence in Molecular Imaging in Cardiovascular and Metabolic Research supported by the Academy of Finland. The work was supported by personal grants from The Finnish Diabetes Research Foundation, Finnish Cultural Foundation Varsinais-Suomi Regional Fund and the Finnish Medical Foundation (A.L-R.). The authors thank Aero Pump GmbH, Hochheim/Main, Germany for kindly providing the nasal pumps used in the study.

CONFLICTS OF INTEREST

Authors have nothing to disclose.

AUTHOR CONTRIBUTIONS

A.L.-R., S.L., H.U.H., M.H. and P.N. designed the study. A.L.-R. and S.L. acquired and analyzed the data. R.K. analyzed metabolite data. T.K. and L.N. contributed to brain data analysis. O.E. is accounted for [^{18}F]-FDG production. A.L.-R., R.K. and E.L. performed statistical analyses. A.L-.R. drafted the manuscript, and all authors participated in editing it. P.N. is the guarantor of this work

and, as such, had full access to all the data in the study and takes responsibility for the integrity of the data and the accuracy of data analysis.

REFERENCES *(currently 44, maximum 60)*

Bartlett, E. J., Brodie, J. D., Wolf, A. P., Christman, D. R., Laska, E., & Meissner, M. (1988). Reproducibility of cerebral glucose metabolic measurements in resting human subjects. *Journal of cerebral blood flow and metabolism : official journal of the International Society of Cerebral Blood Flow and Metabolism*, *8*(4), 502–512.

Benedict C, Brede S, Schiöth HB, Lehnert H, Schultes B, Born J, Hallschmid M. Intranasal insulin enhances postprandial thermogenesis and lowers postprandial serum insulin levels in healthy men. *Diabetes*. 2011;60(1):114-118.

Benomar Y, Naour N, Aubourg A, Bailleux V, Gertler A, Djiane J, Guerre-Millo M, Taouis M. Insulin and leptin induce Glut4 plasma membrane translocation and glucose uptake in a human neuronal cell line by a phosphatidylinositol 3-kinase- dependent mechanism. *Endocrinology*. 2006;147(5):2550-2556.

Bingham, E. M., Hopkins, D., Smith, D., Pernet, A., Hallett, W., Reed, L., Marsden, P. K., & Amiel, S. A. (2002). The role of insulin in human brain glucose metabolism: an 18fluoro-deoxyglucose positron emission tomography study. *Diabetes*, *51*(12), 3384–3390.

Born J, Fehm HL, Kern W, Lange T, Bickel U, McGregor GP. Sniffing neuropeptides: A transnasal approach to the human brain. *Nat Neurosci*. 2002;5(6):514-516.

Coomans CP, Biermasz NR, Geerling JJ, Guigas B, Rensen PCN, Havekes LM, Romijn JA. Stimulatory effect of insulin on glucose uptake by muscle involves the central nervous system in insulin-sensitive mice. *Diabetes*. 2011;60(12):3132-3140.

Dash S, Xiao C, Morgantini C, Koulajian K, Lewis GF. Intranasal insulin suppresses endogenous glucose production in humans compared with placebo in the presence of similar venous insulin concentrations. *Diabetes*. 2015;64(3):766-774.

DeFronzo RA, Tobin JD, Andres R. Glucose clamp technique: A method for quantifying insulin secretion and resistance. *Am J Physiol Endocrinol Metab.* 1979;237(3):214.

Díaz-García CM, Mongeon R, Lahmann C, Koveal D, Zucker H, Yellen G. Neuronal Stimulation Triggers Neuronal Glycolysis and Not Lactate Uptake. *Cell Metab.* 2017 Aug 1;26(2):361-374.e4.

Dienel GA, Wang RY, Cruz NF. Generalized sensory stimulation of conscious rats increases labeling of oxidative pathways of glucose metabolism when the brain glucose-oxygen uptake ratio rises. *J Cereb Blood Flow Metab.* 2002 Dec;22(12):1490-502.

Esterson YB, Carey M, Boucai L, Goyal A, Raghavan P, Zhang K, Mehta D, Feng D, Wu L, Kehlenbrink S, Koppaka S, Kishore P, Hawkins M. Central regulation of glucose production may be impaired in type 2 diabetes. *Diabetes*. 2016;65(9):2569-2579.

Gancheva S, Koliaki C, Bierwagen A, Nowotny P, Heni M, Fritsche A, Häring H, Szendroedi J, Roden M. Effects of intranasal insulin on hepatic fat accumulation and energy metabolism in humans. *Diabetes*. 2015;64(6):1966-1975.

Hamacher K, Coenen HH, Stocklin G. Efficient stereospecific synthesis of no-carrier-added 2-[18F]-fluoro-2-deoxy-D-glucose using aminopolyether supported nucleophilic substitution. *J Nucl Med*. 1986;27(2):235.

Heni M, Hennige AM, Peter A, Siegel-Axel D, Ordelheide A, Krebs N, Machicao F, Fritsche A, Häring H, Staiger H. Insulin promotes glycogen storage and cell proliferation in primary human astrocytes. *PloS one*. 2011;6(6):e21594.

Heni M, Wagner R, Kullmann S, Veit R, Mat Husin H, Linder K, Benkendorff C, Peter A, Stefan N, Häring H, Preissl H, Fritsche A. Central insulin administration improves whole-body insulin sensitivity via hypothalamus and parasympathetic outputs in men. *Diabetes*. 2014;63(12):4083-4088.

Heni M, Wagner R, Kullmann S, Gancheva S, Roden M, Peter A, Stefan N, Preissl H, Häring H, Fritsche A. Hypothalamic and striatal insulin action suppresses endogenous glucose production and may stimulate glucose uptake during hyperinsulinemia in lean but not in overweight men. *Diabetes*. 2017;66(7):1797-1806.

Hirvonen J, Virtanen KA, Nummenmaa L, Hannukainen JC, Honka M, Bucci M, Nesterov SV, Parkkola R, Rinne J, Iozzo P, Nuutila P. Effects of insulin on brain glucose metabolism in impaired glucose tolerance. *Diabetes*. 2011;60(2):443-447.

Iozzo P, Gastaldelli A, Jarvisalo MJ, Kiss J, Borra R, Buzzigoli E, Viljanen A, Naum G, Viljanen T, Oikonen V, Knuuti J, Savunen T, Salvadori PA, Ferrannini E, Nuutila P. 18F-FDG assessment of glucose disposal and production rates during fasting and insulin stimulation: A validation study. *J Nucl Med*. 2006;47(6):1016.

Iozzo P, Jarvisalo MJ, Kiss J, Borra R, Naum GA, Viljanen A, Viljanen T, Gastaldelli A, Buzzigoli E, Guiducci L, Barsotti E, Savunen T, Knuuti J, Haaparanta–Solin M, Ferrannini E, Nuutila P. Quantification of liver glucose metabolism by positron emission tomography: Validation study in pigs. *Gastroenterology*. 2007;132(2):531-542.

Ishibashi K, Wagatsuma K, Ishiwata K, Ishii K. Alteration of the regional cerebral glucose metabolism in healthy subjects by glucose loading. Hum Brain Mapp. 2016 Aug;37(8):2823-32.

Ishizu K, Nishizawa S, Yonekura Y, Sadato N, Magata Y, Tamaki N, Tsuchida T, Okazawa H, Miyatake S, Ishikawa M, Kikuchi H, Konishi J. Effects of hyperglycemia on FDG uptake in human brain and glioma. *J Nucl Med*. 1994;35(7):1104.

Iwen KA, Scherer T, Heni M, Sayk F, Wellnitz T, Machleidt F, Preissl H, Häring H, Fritsche A, Lehnert H, Buettner C, Hallschmid M. Intranasal insulin suppresses systemic but not subcutaneous lipolysis in healthy humans. *J Clin Endocrinol Metab.* 2014;99(2):E246-E251.

Jauch-Chara K, Friedrich A, Rezmer M, Melchert UH, G Scholand-Engler H, Hallschmid M, Oltmanns KM. Intranasal insulin suppresses food intake via enhancement of brain energy levels in humans. *Diabetes.* 2012 Sep;61(9):2261-8.

Karjalainen T, Tuisku J, Santavirta S, Kantonen T, Bucci M, Tuominen L, Hirvonen J, Hietala J, Rinne JO, Nummenmaa L. Magia: Robust automated image processing and kinetic modeling toolbox for PET neuroinformatics. *Front Neuroinform.* 2020 Feb 4;14:3.

Koch L, Wunderlich FT, Seibler J, Könner AC, Hampel B, Irlenbusch S, Brabant G, Kahn CR, Schwenk F, Brüning JC. Central insulin action regulates peripheral glucose and fat metabolism in mice. J Clin Invest. 2008;118(6):2132-2147.

Kullmann S, Kleinridders A, Small DM, Fritsche A, Häring HU, Preissl H, Heni M. Central nervous pathways of insulin action in the control of metabolism and food intake. *Lancet Diabetes Endocrinol*. 2020 Jun;8(6):524-534.

Morgan DA, McDaniel LN, Yin T, Khan M, Jiang J, Acevedo MR, Walsh SA, Ponto LLB, Norris AW, Lutter M, Rahmouni K, Cui H. Regulation of glucose tolerance and sympathetic activity by MC4R signaling in the lateral hypothalamus. *Diabetes*. 2015;64(6):1976-1987.

Obici S, Zhang BB, Karkanias G, Rossetti L. Hypothalamic insulin signaling is required for inhibition of glucose production. *Nat Med*. 2002;8(12):1376-1382.

Patlak CS, Blasberg RG. Graphical evaluation of blood-to-brain transfer constants from multiple-time uptake data. generalizations. *J Cereb Blood Flow Metab*. 1985;5(4):584-590.

Peltoniemi P, Lönnroth P, Laine H, Oikonen V, Tolvanen T, Grönroos T, Strindberg L, Knuuti J, Nuutila P. Lumped constant for [(18)F]fluorodeoxyglucose in skeletal muscles of obese and nonobese humans. *Am J Physiol Endocrinol Metab.* 2000 Nov;279(5):E1122-30.

Perrin C, Knauf C, Burcelin R. Intracerebroventricular infusion of glucose, insulin, and the adenosine monophosphate-activated kinase activator, 5-aminoimidazole-4-carboxamide-1-β-d-ribofuranoside, controls muscle glycogen synthesis. *Endocrinology*. 2004;145(9):4025-4033.

Plomgaard P, Hansen JS, Ingerslev B, Clemmesen JO, Secher NH, van Hall G, Fritsche A, Weigert C, Lehmann R, Häring H, Heni M. Nasal insulin administration does not affect hepatic glucose production at systemic fasting insulin levels. *Diabetes Obes Metab*. 2019;21(4):993-1000.

Pocai A, Lam TKT, Gutierrez-Juarez R, Obici S, Schwartz GJ, Bryan J, Aguilar-Bryan L, Rossetti L. Hypothalamic KATP channels control hepatic glucose production. *Nature*. 2005;434(7036):1026-1031.

Rahmouni K, Morgan DA, Morgan GM, Liu X, Sigmund CD, Mark AL, Haynes WG. Hypothalamic PI3K and MAPK differentially mediate regional sympathetic activation to insulin. *J Clin Invest*. 2004;114(5):652-658.

Ramnanan CJ, Saraswathi V, Smith MS, Donahue EP, Farmer B, Farmer TD, Neal D, Williams PE, Lautz M, Mari A, Cherrington AD, Edgerton DS. Brain insulin action augments hepatic glycogen synthesis without suppressing glucose production or gluconeogenesis in dogs. *J Clin Invest*. 2011 Sep;121(9):3713-23.

Renner DB, Svitak AL, Gallus NJ, Ericson ME, Frey WH, Hanson LR. Intranasal delivery of insulin via the olfactory nerve pathway. *J Pharm Pharmacol*. 2012;64(12):1709-1714.

Reno CM, Puente EC, Sheng Z, Daphna-Iken D, Bree AJ, Routh VH, Kahn BB, Fisher SJ. Brain GLUT4 knockout mice have impaired glucose tolerance, decreased insulin sensitivity, and impaired hypoglycemic counterregulation. *Diabetes*. 2017;66(3):587-597.

Sanguinetti E, Guzzardi MA, Panetta D, Tripodi M, De Sena V, Quaglierini M, Burchielli S, Salvadori PA, Iozzo P. Combined effect of fatty diet and cognitive decline on brain metabolism, food intake, body weight, and counteraction by intranasal insulin therapy in 3×Tg mice. *Front Cell Neurosci*. 2019;13:188.

Scherer T, O'Hare J, Diggs-Andrews K, Schweiger M, Cheng B, Lindtner C, Zielinski E, Vempati P, Su K, Dighe S, Milsom T, Puchowicz M, Scheja L, Zechner R, Fisher SJ, Previs SF, Buettner C. Brain insulin controls adipose tissue lipolysis and lipogenesis. *Cell Metab*. 2011;13(2):183-194.

Scherer, T., Sakamoto, K. & Buettner, C. Brain insulin signalling in metabolic homeostasis and disease. *Nat Rev Endocrinol.* 2021;17:468–483.

Soininen P, Kangas AJ, Würtz P, Tukiainen T, Tynkkynen T, Laatikainen R, Järvelin M, Kähönen M, Lehtimäki T, Viikari J, Raitakari OT, Savolainen MJ, Ala-Korpela M. High-throughput serum NMR metabonomics for cost-effective holistic studies on systemic metabolism. *Analyst*. 2009;134(9):1781-1785.

Virtanen KA, Peltoniemi P, Marjamäki P, Asola M, Strindberg L, Parkkola R, Huupponen R, Knuuti J, Lönnroth P, Nuutila P. Human adipose tissue glucose uptake determined using [18F]-fluoro-deoxy-glucose ([18F]FDG) and PET in combination with microdialysis. *Diabetologia*. 2001;44(12):2171-2179.

Wu H, Bergsneider M, Glenn TC, Yeh E, Hovda DA, Phelps ME, Huang S. Measurement of the global lumped constant for 2-deoxy-2-[18F]fluoro-D-glucose in normal human brain using [15O]water and 2-deoxy-2-[18F]fluoro-D-glucose positron emission tomography imaging : A method with validation based on multiple methodologies. *Mol Imaging Biol*. 2003;5(1):32-41.

Xiao C, Dash S, Stahel P, Lewis G. Effects of intranasal insulin on triglyceride-rich lipoprotein particle production in healthy men. *Arterioscler Thromb Vasc* Biol. 2017;37(9):1776-1781.

Xiao C, Dash S, Stahel P, Lewis GF. Effects of intranasal insulin on endogenous glucose production in insulin-resistant men. *Diabetes Obes Metab*. 2018;20(7):1751-1754.

	Whole group (N=10)		High sensitivity (N=5)		Impaired sensitivity (N=5)	
	Mean	Range	Mean	Range	Mean	Range
Age (y)	24	20–28	26	24–28	22	20-24
Weight (kg)	76.8	65.2–87.5	80.1	74.3–87.5	73.5	65.2–82.0
BMI (kg/m^2)	23.5	20.0–25.6	24.5	22.6–25.6	22.5	20.0–25.0
Fat percentage (%)	16.5	9.7–20.3	18.3	15.3–20.3	14.7	9.7–19.7
Waist-to-hip ratio	0.84	0.80–0.91	0.84	0.82–0.87	0.84	0.80–0.91
Fasting plasma glucose (mmol/L)	5.2	3.7–5.8	5.2	3.7–5.8	5.2	4.7–5.4
HbA1c (mmol/mol)	29	24–32	29	24–32	29	25–32
HbA1c (%)	4,8	(4,3–5,1)	4,8	(4,3–5,1)	4,8	(4,4–5,1)
Fasting plasma insulin (pmol/L)	35	7–69	25	7–41	53	35–69
Matsuda-ISI	9.4	3. –27.2	13.6	8.2–27.2	5.1	3.5–6.5

Table 1. Subject characteristics for the whole group, and subgroups based on peripheral insulin sensitivity (Matsuda-ISI ≥7.4 or <7.4).

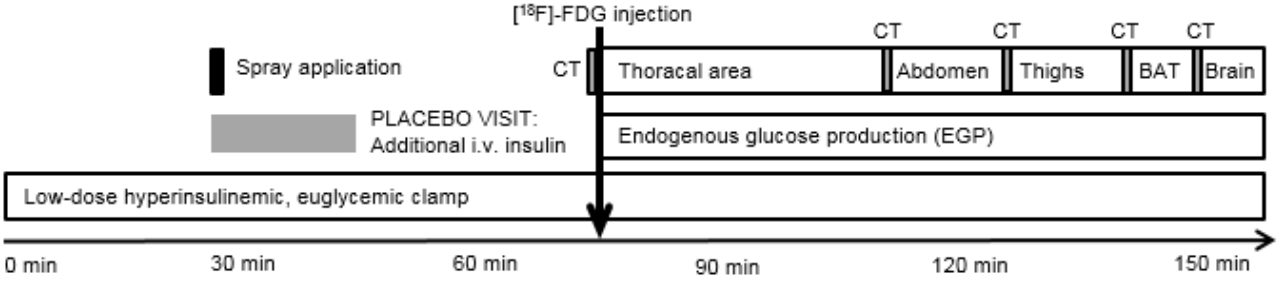

Figure 1. Experimental protocol.

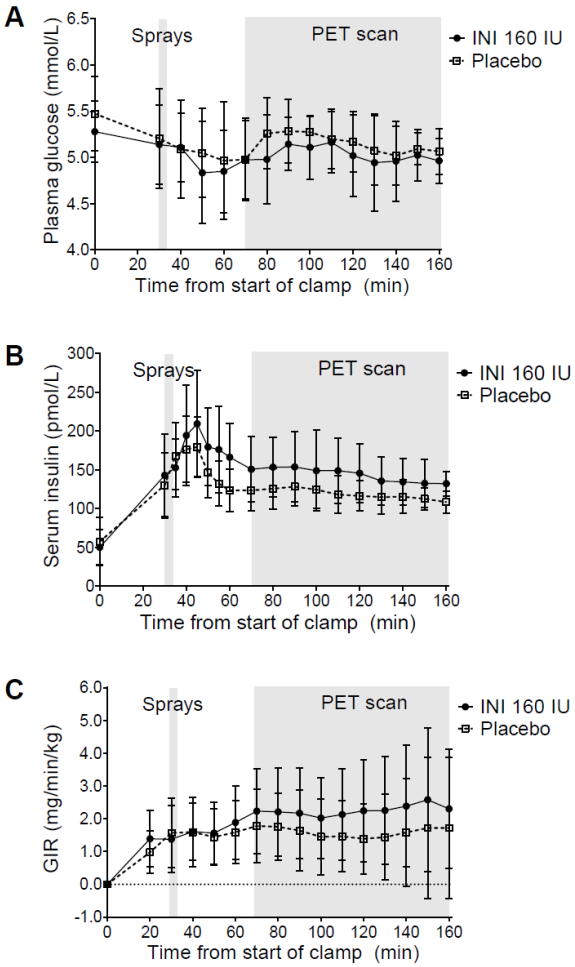

Figure 2. A, Plasma glucose (mmol/L); and B, serum insulin (pmol/L) concentrations during the studies. C, Glucose infusion rate (GIR, mg kg^{-1} min^{-1}) during the studies. Data are mean and SD. The gray background represents the 4-minute period of spray application at 30 minutes, and the PET scan periods.

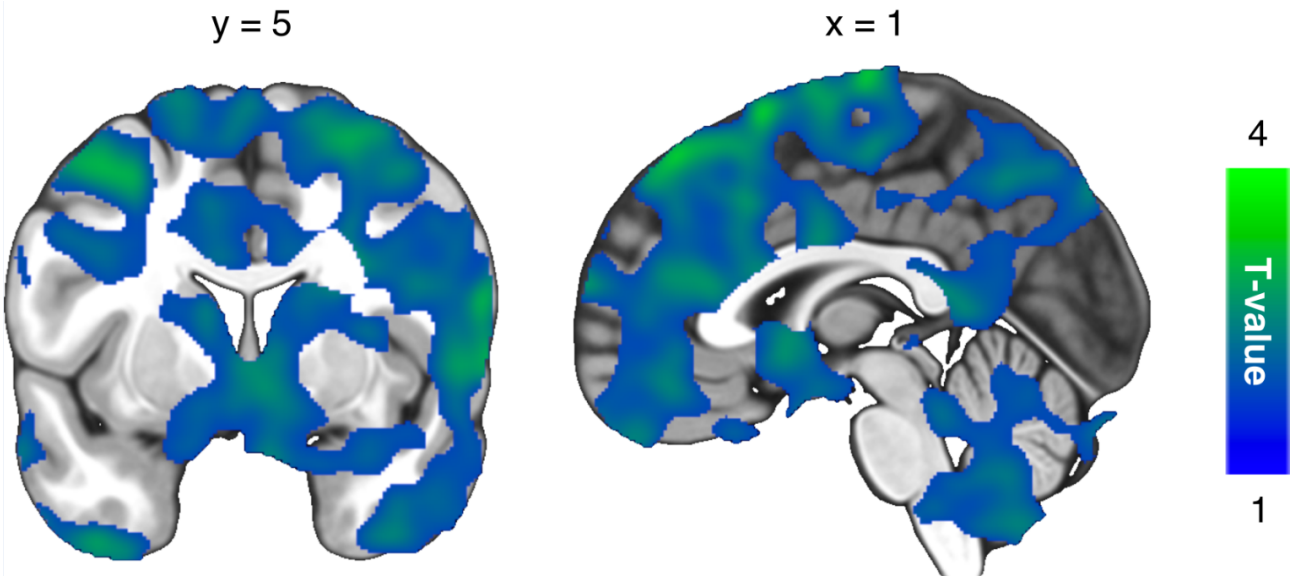

Figure 3. Compared to placebo, INI lowered brain GU globally. The data are thresholded at p< 0.05, FWE-corrected at cluster level. The x and y coordinates refer to the neuroanatomical locations of the slices in the MNI space.

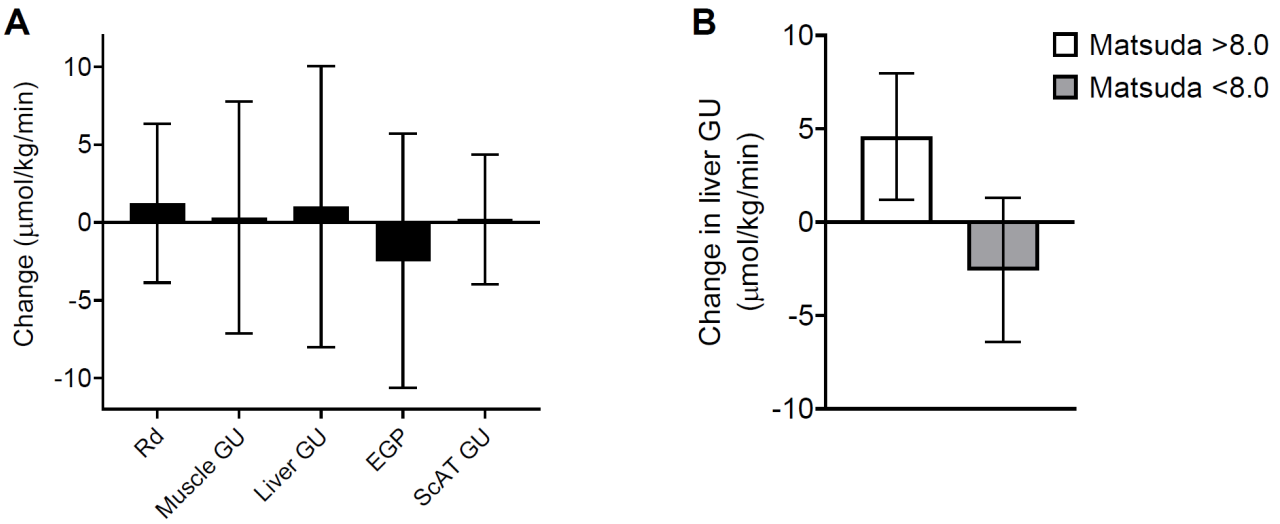

Figure 4. A. Changes in rates of [^{18}F]-FDG-derived glucose disappearance (Rd), tissue glucose uptake (GU) in skeletal muscle, liver and subcutaneous adipose tissue (ScAT), and endogenous glucose production (EGP) after intranasal insulin compared to placebo. B. Comparison of INI induced changes in liver GU in subjects with high (Matsuda-ISI ≥7.4, white bar) or low (Matsuda-ISI <7.4, grey bar) insulin sensitivity. Bars represent means, vertical lines CIs.